Suppressed π^0 Production at Large Transverse Momentum in Central Au + Au Collisions at $\sqrt{s_{NN}} = 200$ GeV

S. S. Adler,[5] S. Afanasiev,[17] C. Aidala,[5] N. N. Ajitanand,[43] Y. Akiba,[20,38] J. Alexander,[43] R. Amirikas,[12] L. Aphecetche,[45] S. H. Aronson,[5] R. Averbeck,[44] T. C. Awes,[35] R. Azmoun,[44] V. Babintsev,[15] A. Baldisseri,[10] K. N. Barish,[6] P. D. Barnes,[27] B. Bassalleck,[33] S. Bathe,[30] S. Batsouli,[9] V. Baublis,[37] A. Bazilevsky,[39,15] S. Belikov,[16,15] Y. Berdnikov,[40] S. Bhagavatula,[16] J. G. Boissevain,[27] H. Borel,[10] S. Borenstein,[25] M. L. Brooks,[27] D. S. Brown,[34] N. Bruner,[33] D. Bucher,[30] H. Buesching,[30] V. Bumazhnov,[15] G. Bunce,[5,39] J. M. Burward-Hoy,[26,44] S. Butsyk,[44] X. Camard,[45] J.-S. Chai,[18] P. Chand,[4] W. C. Chang,[2] S. Chernichenko,[15] C. Y. Chi,[9] J. Chiba,[20] M. Chiu,[9] I. J. Choi,[52] J. Choi,[19] R. K. Choudhury,[4] T. Chujo,[5] V. Cianciolo,[35] Y. Cobigo,[10] B. A. Cole,[9] P. Constantin,[16] D. G. d'Enterria,[45] G. David,[5] H. Delagrange,[45] A. Denisov,[15] A. Deshpande,[39] E. J. Desmond,[5] O. Dietzsch,[41] O. Drapier,[25] A. Drees,[44] K. A. Drees,[5] R. du Rietz,[29] A. Durum,[15] D. Dutta,[4] Y. V. Efremenko,[35] K. El Chenawi,[49] A. Enokizono,[14] H. En'yo,[38,39] S. Esumi,[48] L. Ewell,[5] D. E. Fields,[33,39] F. Fleuret,[25] S. L. Fokin,[23] B. D. Fox,[39] Z. Fraenkel,[51] J. E. Frantz,[9] A. Franz,[5] A. D. Frawley,[12] S.-Y. Fung,[6] S. Garpman,[29,*] T. K. Ghosh,[49] A. Glenn,[46] G. Gogiberidze,[46] M. Gonin,[25] J. Gosset,[10] Y. Goto,[39] R. Granier de Cassagnac,[25] N. Grau,[16] S. V. Greene,[49] M. Grosse Perdekamp,[39] W. Guryn,[5] H.-Å. Gustafsson,[29] T. Hachiya,[14] J. S. Haggerty,[5] H. Hamagaki,[8] A. G. Hansen,[27] E. P. Hartouni,[26] M. Harvey,[5] R. Hayano,[8] X. He,[13] M. Heffner,[26] T. K. Hemmick,[44] J. M. Heuser,[44] M. Hibino,[50] J. C. Hill,[16] W. Holzmann,[43] K. Homma,[14] B. Hong,[22] A. Hoover,[34] T. Ichihara,[38,39] V. V. Ikonnikov,[23] K. Imai,[24,38] L. Isenhower,[1] M. Ishihara,[38] M. Issah,[43] A. Isupov,[17] B. V. Jacak,[44] W. Y. Jang,[22] Y. Jeong,[19] J. Jia,[44] O. Jinnouchi,[38] B. M. Johnson,[5] S. C. Johnson,[26] K. S. Joo,[31] D. Jouan,[36] S. Kametani,[8,50] N. Kamihara,[47,38] J. H. Kang,[52] S. S. Kapoor,[4] K. Katou,[50] S. Kelly,[9] B. Khachaturov,[51] A. Khanzadeev,[37] J. Kikuchi,[50] D. H. Kim,[31] D. J. Kim,[52] D. W. Kim,[19] E. Kim,[42] G.-B. Kim,[25] H. J. Kim,[52] E. Kistenev,[5] A. Kiyomichi,[48] K. Kiyoyama,[32] C. Klein-Boesing,[30] H. Kobayashi,[38,39] L. Kochenda,[37] V. Kochetkov,[15] D. Koehler,[33] T. Kohama,[14] M. Kopytine,[44] D. Kotchetkov,[6] A. Kozlov,[51] P. J. Kroon,[5] C. H. Kuberg,[1,27] K. Kurita,[39] Y. Kuroki,[48] M. J. Kweon,[22] Y. Kwon,[52] G. S. Kyle,[34] R. Lacey,[43] V. Ladygin,[17] J. G. Lajoie,[16] A. Lebedev,[16,23] S. Leckey,[44] D. M. Lee,[27] S. Lee,[19] M. J. Leitch,[27] X. H. Li,[6] H. Lim,[42] A. Litvinenko,[17] M. X. Liu,[27] Y. Liu,[36] C. F. Maguire,[49] Y. I. Makdisi,[5] A. Malakhov,[17] V. I. Manko,[23] Y. Mao,[7,38] G. Martinez,[45] M. D. Marx,[44] H. Masui,[48] F. Matathias,[44] T. Matsumoto,[8,50] P. L. McGaughey,[27] E. Melnikov,[15] F. Messer,[44] Y. Miake,[48] J. Milan,[43] T. E. Miller,[49] A. Milov,[44,51] S. Mioduszewski,[5] R. E. Mischke,[27] G. C. Mishra,[13] J. T. Mitchell,[5] A. K. Mohanty,[4] D. P. Morrison,[5] J. M. Moss,[27] F. Mühlbacher,[44] D. Mukhopadhyay,[51] M. Muniruzzaman,[6] J. Murata,[38,39] S. Nagamiya,[20] J. L. Nagle,[9] T. Nakamura,[14] B. K. Nandi,[6] M. Nara,[48] J. Newby,[46] P. Nilsson,[29] A. S. Nyanin,[23] J. Nystrand,[29] E. O'Brien,[5] C. A. Ogilvie,[16] H. Ohnishi,[5,38] I. D. Ojha,[49,3] K. Okada,[38] M. Ono,[48] V. Onuchin,[15] A. Oskarsson,[29] I. Otterlund,[29] K. Oyama,[8] K. Ozawa,[8] D. Pal,[51] A. P. T. Palounek,[27] V. S. Pantuev,[44] V. Papavassiliou,[34] J. Park,[42] A. Parmar,[33] S. F. Pate,[34] T. Peitzmann,[30] J.-C. Peng,[27] V. Peresedov,[17] C. Pinkenburg,[5] R. P. Pisani,[5] F. Plasil,[35] M. L. Purschke,[5] A. K. Purwar,[44] J. Rak,[16] I. Ravinovich,[51] K. F. Read,[35,46] M. Reuter,[44] K. Reygers,[30] V. Riabov,[37,40] Y. Riabov,[37] G. Roche,[28] A. Romana,[25] M. Rosati,[16] P. Rosnet,[28] S. S. Ryu,[52] M. E. Sadler,[1] N. Saito,[38,39] T. Sakaguchi,[8,50] M. Sakai,[32] S. Sakai,[48] V. Samsonov,[37] L. Sanfratello,[33] R. Santo,[30] H. D. Sato,[24,38] S. Sato,[5,48] S. Sawada,[20] Y. Schutz,[45] V. Semenov,[15] R. Seto,[6] M. R. Shaw,[1,27] T. K. Shea,[5] T.-A. Shibata,[47,38] K. Shigaki,[14,20] T. Shiina,[27] C. L. Silva,[41] D. Silvermyr,[27,29] K. S. Sim,[22] C. P. Singh,[3] V. Singh,[3] M. Sivertz,[5] A. Soldatov,[15] R. A. Soltz,[26] W. E. Sondheim,[27] S. P. Sorensen,[46] I. V. Sourikova,[5] F. Staley,[10] P. W. Stankus,[35] E. Stenlund,[29] M. Stepanov,[34] A. Ster,[21] S. P. Stoll,[5] T. Sugitate,[14] J. P. Sullivan,[27] E. M. Takagui,[41] A. Taketani,[38,39] M. Tamai,[50] K. H. Tanaka,[20] Y. Tanaka,[32] K. Tanida,[38] M. J. Tannenbaum,[5] P. Tarján,[11] J. D. Tepe,[1,27] T. L. Thomas,[33] J. Tojo,[24,38] H. Torii,[24,38] R. S. Towell,[1] I. Tserruya,[51] H. Tsuruoka,[48] S. K. Tuli,[3] H. Tydesjö,[29] N. Tyurin,[15] H. W. van Hecke,[27] J. Velkovska,[5,44] M. Velkovsky,[44] L. Villatte,[46] A. A. Vinogradov,[23] M. A. Volkov,[23] E. Vznuzdaev,[37] X. R. Wang,[13] Y. Watanabe,[38,39] S. N. White,[5] F. K. Wohn,[16] C. L. Woody,[5] W. Xie,[6] Y. Yang,[7] A. Yanovich,[15] S. Yokkaichi,[38,39] G. R. Young,[35] I. E. Yushmanov,[23] W. A. Zajc,[9,†] C. Zhang,[9] S. Zhou,[7,51] and L. Zolin[17]

(PHENIX Collaboration)

[1]*Abilene Christian University, Abilene, Texas 79699, USA*
[2]*Institute of Physics, Academia Sinica, Taipei 11529, Taiwan*
[3]*Department of Physics, Banaras Hindu University, Varanasi 221005, India*

 0031-9007/03/91(7)/072301(6)$20.00

[4]*Bhabha Atomic Research Centre, Bombay 400 085, India*
[5]*Brookhaven National Laboratory, Upton, New York 11973-5000, USA*
[6]*University of California–Riverside, Riverside, California 92521, USA*
[7]*China Institute of Atomic Energy (CIAE), Beijing, People's Republic of China*
[8]*Center for Nuclear Study, Graduate School of Science, University of Tokyo, 7-3-1 Hongo, Bunkyo, Tokyo 113-0033, Japan*
[9]*Columbia University, New York, New York 10027, USA, and Nevis Laboratories, Irvington, New York 10533, USA*
[10]*Dapnia, CEA Saclay, F-91191, Gif-sur-Yvette, France*
[11]*Debrecen University, H-4010 Debrecen, Egyetem tér 1, Hungary*
[12]*Florida State University, Tallahassee, Florida 32306, USA*
[13]*Georgia State University, Atlanta, Georgia 30303, USA*
[14]*Hiroshima University, Kagamiyama, Higashi-Hiroshima 739-8526, Japan*
[15]*Institute for High Energy Physics (IHEP), Protvino, Russia*
[16]*Iowa State University, Ames, Iowa 50011, USA*
[17]*Joint Institute for Nuclear Research, 141980 Dubna, Moscow Region, Russia*
[18]*KAERI, Cyclotron Application Laboratory, Seoul, South Korea*
[19]*Kangnung National University, Kangnung 210-702, South Korea*
[20]*KEK, High Energy Accelerator Research Organization, Tsukuba-shi, Ibaraki-ken 305-0801, Japan*
[21]*KFKI Research Institute for Particle and Nuclear Physics (RMKI), H-1525 Budapest 114, PO Box 49, Hungary*
[22]*Korea University, Seoul, 136-701, Korea*
[23]*Russian Research Center, "Kurchatov Institute," Moscow, Russia*
[24]*Kyoto University, Kyoto 606, Japan*
[25]*Laboratoire Leprince-Ringuet, Ecole Polytechnique, CNRS-IN2P3, Route de Saclay, F-91128, Palaiseau, France*
[26]*Lawrence Livermore National Laboratory, Livermore, California 94550, USA*
[27]*Los Alamos National Laboratory, Los Alamos, New Mexico 87545, USA*
[28]*LPC, Université Blaise Pascal, CNRS-IN2P3, Clermont-Fd, 63177 Aubiere Cedex, France*
[29]*Department of Physics, Lund University, Box 118, SE-221 00 Lund, Sweden*
[30]*Institut fuer Kernphysik, University of Muenster, D-48149 Muenster, Germany*
[31]*Myongji University, Yongin, Kyonggido 449-728, Korea*
[32]*Nagasaki Institute of Applied Science, Nagasaki-shi, Nagasaki 851-0193, Japan*
[33]*University of New Mexico, Albuquerque, New Mexico 87131, USA*
[34]*New Mexico State University, Las Cruces, New Mexico 88003, USA*
[35]*Oak Ridge National Laboratory, Oak Ridge, Tennessee 37831, USA*
[36]*IPN-Orsay, Universite Paris Sud, CNRS-IN2P3, BP1, F-91406, Orsay, France*
[37]*PNPI, Petersburg Nuclear Physics Institute, Gatchina, Russia*
[38]*RIKEN (The Institute of Physical and Chemical Research), Wako, Saitama 351-0198, Japan*
[39]*RIKEN BNL Research Center, Brookhaven National Laboratory, Upton, New York 11973-5000*
[40]*St. Petersburg State Technical University, St. Petersburg, Russia*
[41]*Universidade de São Paulo, Instituto de Física, Caixa Postal 66318, São Paulo CEP05315-970, Brazil*
[42]*System Electronics Laboratory, Seoul National University, Seoul, South Korea*
[43]*Chemistry Department, Stony Brook University, SUNY, Stony Brook, New York 11794-3400, USA*
[44]*Department of Physics and Astronomy, Stony Brook University, SUNY, Stony Brook, New York 11794, USA*
[45]*SUBATECH (Ecole des Mines de Nantes, CNRS-IN2P3, Université de Nantes) BP 20722-44307, Nantes, France*
[46]*University of Tennessee, Knoxville, Tennessee 37996, USA*
[47]*Department of Physics, Tokyo Institute of Technology, Tokyo, 152-8551, Japan*
[48]*Institute of Physics, University of Tsukuba, Tsukuba, Ibaraki 305, Japan*
[49]*Vanderbilt University, Nashville, Tennessee 37235, USA*
[50]*Waseda University, Advanced Research Institute for Science and Engineering, 17 Kikui-cho, Shinjuku-ku, Tokyo 162-0044, Japan*
[51]*Weizmann Institute, Rehovot 76100, Israel*
[52]*Yonsei University, IPAP, Seoul 120-749, Korea*
(Received 28 April 2003; published 13 August 2003)

Transverse momentum spectra of neutral pions in the range $1 < p_T < 10$ GeV/c have been measured at midrapidity by the PHENIX experiment at BNL RHIC in Au + Au collisions at $\sqrt{s_{NN}} = 200$ GeV. The π^0 multiplicity in central reactions is significantly below the yields measured at the same $\sqrt{s_{NN}}$ in peripheral Au + Au and $p + p$ reactions scaled by the number of nucleon-nucleon collisions. For the most central bin, the suppression factor is ~2.5 at $p_T = 2$ GeV/c and increases to ~4–5 at $p_T \approx 4$ GeV/c. At larger p_T, the suppression remains constant within errors. The deficit is already apparent in semiperipheral reactions and increases smoothly with centrality.

DOI: 10.1103/PhysRevLett.91.072301 PACS numbers: 25.75.Dw

High energy collisions of heavy ions provide the means to study quantum chromodynamics (QCD) at energy densities where lattice calculations [1] predict a transition from hadronic matter to a deconfined, chirally symmetric plasma of quarks and gluons (QGP). The large center-of-mass energies, $\sqrt{s_{NN}} \approx 200$ GeV, available in Au + Au collisions at the BNL Relativistic Heavy Ion Collider (RHIC), have resulted in a significant production of high transverse momentum hadrons ($p_T > 2$ GeV/c) for the first time in heavy-ion physics. High p_T particle production in hadronic collisions results from the fragmentation of quarks and gluons emerging from the initial high Q^2 parton-parton scatterings [2]. Thus, hard processes in nucleus-nucleus (AA) collisions provide direct information on the early partonic phases of the reaction. In the absence of nuclear medium effects, hard scattering yields in AA reactions are expected to scale like an incoherent superposition of nucleon-nucleon (NN) collisions because of the small probability of hard scattering processes per NN collision. In AA reactions, the number of NN collisions ($N_{\rm coll}$) at impact parameter b is simply proportional to the geometric nuclear overlap function, $T_{AA}(b)$, and can be calculated in an eikonal approach [3]. After scaling by the nuclear geometry, spectra of high p_T particles measured in AA reactions can be compared to the baseline $p + p$, $p + A$ data, as well as to perturbative [4–7] and classical-field [8] QCD predictions. Any departure from the expected $N_{\rm coll}$-scaled result provides information on the strongly interacting medium in central heavy-ion reactions.

One of the most significant observations from the first RHIC run (run 1) was the suppressed yield of moderately high p_T neutral pions ($p_T \approx 1.5$–4.0 GeV/c) in central Au + Au at $\sqrt{s_{NN}} = 130$ GeV with respect to the $N_{\rm coll}$-scaled $p + p$ and peripheral Au + Au data [9]. This result points to strong medium effects present in central Au + Au and has triggered extensive theoretical studies on its origin [4–8,10–13]. Most of these studies are based on the prediction [14,15] that a QGP would induce multiple gluon radiations from the scattered fast partons, effectively leading to a suppression of high p_T hadronic fragmentation products ("jet quenching"). Alternative interpretations have been proposed based on initial-state gluon saturation [8] or final-state hadronic interactions [13].

This Letter presents π^0 results obtained by the PHENIX experiment in Au + Au collisions at $\sqrt{s_{NN}} =$ 200 GeV and compares them to the $p + p \to \pi^0 X$ data measured in the same experiment at the same center-of-mass energy [16]. The analysis uses 30×10^6 minimum bias events, triggered by a coincidence between the zero degree calorimeters (ZDC) and the beam-beam counters (BBC), with vertex position $|z| < 30$ cm. In run 2, the electromagnetic calorimeter (EMCal) was fully instrumented providing a total solid angle coverage at midrapidity of approximately $\Delta\eta = 0.7$ and $\Delta\phi = \pi$ and the total collected π^0 statistics was a factor of $\sim$100 larger than in run 1 [9]. The combination of larger acceptance, high statistics, and the measurement of $p + p$ data in the same detector permits a precise study of the high p_T π^0 production mechanisms in AA collisions at RHIC.

Neutral pions are reconstructed via their $\pi^0 \to \gamma\gamma$ decay through an invariant mass analysis of γ pairs detected in the EMCal [17] which consists of six lead-scintillator (PbSc) and two lead-glass Čerenkov (PbGl) sectors. The large radial distance of the calorimeters to the interaction region (> 5 m) and their fine granularity ($\Delta\eta \times \Delta\phi \approx 0.01 \times 0.01$) keep the tower occupancy low, $<10\%$ even in the highest multiplicity Au + Au events. The energy calibration is obtained from beam tests and, in the case of PbSc, from cosmic rays data and the known minimum ionizing energy peak of charged hadrons traversing the calorimeter. It is then confirmed using the π^0 mass, as well as the agreement of the calorimeter energy with the measured momentum of identified electrons. The systematic error on the absolute energy scale is less than 1.5%. Photonlike clusters are identified in the EMCal by applying time-of-flight and shower profile cuts [17]. The selected clusters are binned in pair invariant mass $m_{\gamma\gamma}$ and p_T. An additional energy asymmetry cut, $|E_{\gamma 1} - E_{\gamma 2}|/(E_{\gamma 1} + E_{\gamma 2}) <$ 0.7(PbGl), 0.8(PbSc), is applied to the reconstructed pairs. The signal-to-background in peripheral (central) is approximately 20 (5) and 0.5 (0.01) for the highest and lowest p_T, respectively. The combinatorial background is estimated and subtracted by mixing clusters from different events with similar centrality and vertex, and normalizing the distribution in a region outside the π^0 mass peak. The π^0 yield in each p_T bin is determined by integrating the subtracted $m_{\gamma\gamma}$ distribution in a $\pm 3\sigma$ window determined by a p_T-dependent parametrization of Gaussian fits to the π^0 peaks.

The raw PbSc and PbGl π^0 spectra are normalized to one unit of rapidity and full azimuth (this acceptance correction quickly reaches the $\sim 1/0.35$ pure geometric factor at high p_T). The spectra are further corrected for (i) the detector response (energy resolution, dead areas), (ii) the reconstruction efficiency (analysis cuts), and (iii) the occupancy effects (cluster overlaps). These corrections are quantified by embedding simulated single π^0's from a full PHENIX GEANT [18] simulation into real events, and analyzing the merged events with the same analysis cuts used to obtain the real yields. Each correction is determined, for each centrality bin, as the ratio of the input to the reconstructed simulated p_T distributions. The overall yield correction amounts to $\sim$2.5 with a centrality dependence $\lesssim 25\%$. The losses are dominated by fiducial and asymmetry cuts.

The main sources of systematic errors in the PbSc and PbGl measurements are due to the uncertainties in (i) the yield extraction (background subtraction and $m_{\rm inv}$ integration), (ii) the yield correction (efficiency factors), and

TABLE I. Summary of the dominant sources of systematic errors on the PbSc and PbGl π^0 yields and total errors on the combined measurements. The error ranges are quoted for the lowest to highest p_T values.

Source		Syst. error PbSc	Syst. error PbGl	
Yield extraction		10%	6%–7%	
Yield correction		8%	8%	
Energy scale		3%–11%	7%–13%	
Total error (%)	Stat.	Syst.	Normalization Central	Peripheral
Comb. π^0 spectra	2–40	10–17	5	5
R_{AA}	2–45	11–22	14	30

(iii) the energy scale (absolute calibration of the calorimeter). The relative contributions of these effects to the total error differ for the PbSc and PbGl (Table I). The weighted average of the two independent measurements reduces the total error. The nominal energy resolution [17] is adjusted in the simulation to reproduce the true width of the π^0 peak observed at each p_T, smearing the energies with a constant term of 7% for PbSc and ~9% for PbGl. The shape, position, and width of the π^0 peak measured in all different centralities are then confirmed to be well reproduced by the embedded data. The final systematic errors on the spectra are at the level of ~10% at 1 GeV/c and ~17% at the highest p_T (Table I). A correction for the true mean value of the p_T bin is applied to the steeply falling spectra. No corrections have been applied to account for the contribution of feed-down π^0's (mainly coming from K^0_s and η decays) which are <5% based on HIJING [19] simulations.

The event centrality is determined by correlating the charge detected in the BBC with the energy measured in the ZDC detectors. A Glauber model Monte Carlo (MC) calculation combined with a simulation of the BBC and ZDC responses [20–22] gives an estimate of the associated averaged number of binary collisions ($\langle N_{\rm coll}\rangle$) and participating nucleons ($\langle N_{\rm part}\rangle$) in each centrality bin (Table II). Fully corrected and combined PbSc and PbGl π^0 p_T distributions are shown in Fig. 1 for minimum bias and for nine centrality bins scaled by factors of 10.

We quantify the medium effects on high p_T production in AA collisions with the *nuclear modification factor* given by the ratio of the measured AA invariant yields to the NN collision scaled $p + p$ invariant yields:

$$R_{AA}(p_T) = \frac{(1/N^{\rm evt}_{AA}) d^2N^{\pi^0}_{AA}/dp_T dy}{\langle N_{\rm coll}\rangle/\sigma^{\rm inel}_{pp} \times d^2\sigma^{\pi^0}_{pp}/dp_T dy}, \quad (1)$$

where the $\langle N_{\rm coll}\rangle/\sigma^{\rm inel}_{pp}$ is just the average Glauber nuclear overlap function, $\langle T_{\rm AuAu}\rangle$, in the centrality bin under consideration (Table II). $R_{AA}(p_T)$ measures the deviation of AA data from an incoherent superposition of NN collisions. For $p_T \lesssim 2$ GeV/c, R_{AA} is known to be below unity, since the bulk of particle production is due to soft processes which scale closer to the number of participant nucleons [20] than to $\langle N_{\rm coll}\rangle$.

TABLE II. Centrality bin, average nuclear overlap function, number of NN collisions, and number of participant nucleons from a Glauber MC [21,22] and the BBC and ZDC responses for Au + Au at $\sqrt{s_{NN}} = 200$ GeV. The centrality bin is expressed as percentiles of $\sigma_{\rm AuAu} = 6.9$ b.

Centrality	$\langle T_{\rm AuAu}\rangle$ (mb^{-1})	$\langle N_{\rm coll}\rangle$	$\langle N_{\rm part}\rangle$
0%–10%	22.75 ± 1.56	955.4 ± 93.6	325.2 ± 3.3
10%–20%	14.35 ± 1.00	602.6 ± 59.3	234.6 ± 4.7
20%–30%	8.90 ± 0.72	373.8 ± 39.6	166.6 ± 5.4
30%–40%	5.23 ± 0.44	219.8 ± 22.6	114.2 ± 4.4
40%–50%	2.86 ± 0.28	120.3 ± 13.7	74.4 ± 3.8
50%–60%	1.45 ± 0.23	61.0 ± 9.9	45.5 ± 3.3
60%–70%	0.68 ± 0.18	28.5 ± 7.6	25.7 ± 3.8
60%–80%	0.49 ± 0.14	20.4 ± 5.9	19.5 ± 3.3
60%–92%	0.35 ± 0.10	14.5 ± 4.0	14.5 ± 2.5
70%–80%	0.30 ± 0.10	12.4 ± 4.2	13.4 ± 3.0
70%–92%	0.20 ± 0.06	8.3 ± 2.4	9.5 ± 1.9
80%–92%	0.12 ± 0.03	4.9 ± 1.2	6.3 ± 1.2
Min. bias	6.14 ± 0.45	257.8 ± 25.4	109.1 ± 4.1

Figure 2 shows R_{AA} as a function of p_T for π^0 measured in 0%–10% central (closed circles) and 80%–92% peripheral (open circles) Au + Au. The PHENIX $p + p \rightarrow \pi^0$ data [16] is used as the reference in the denominator. The R_{AA} values for central collisions are noticeably below unity, as found at 130 GeV [9]. This is in contrast to the enhanced high p_T π^0 production ($R_{AA} > 1$) observed

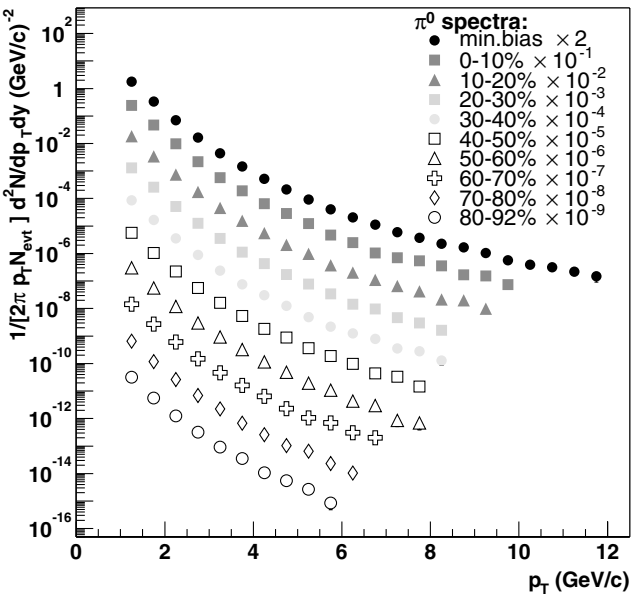

FIG. 1. Invariant π^0 yields at midrapidity as a function of p_T for minimum bias and nine centralities in Au + Au at $\sqrt{s_{NN}} = 200$ GeV [0%–10% (80%–92%) is most central (peripheral)].

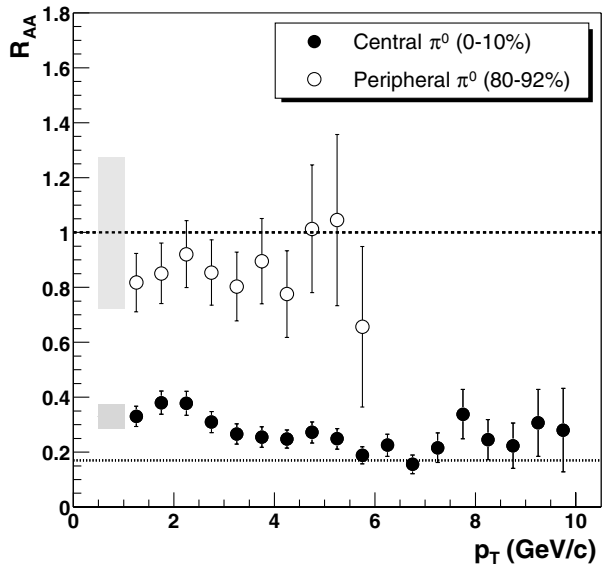

FIG. 2. Nuclear modification factor $R_{AA}(p_T)$ for π^0 in central (closed circles) and peripheral (open circles) Au + Au at $\sqrt{s_{NN}} = 200$ GeV. The error bars include all point-to-point experimental ($p + p$, Au + Au) errors. The shaded bands represent the fractional uncertainties in $\langle T_{\mathrm{AuAu}} \rangle$ and in the π^0 yields normalization added in quadrature, which can move all the points up or down together (in the central case the shaded band shown is the fractional error for the first point).

at CERN Super Proton Synchrotron energies [23], interpreted in terms of initial-state p_T broadening effects ("Cronin effect" [24]). Within errors, peripheral Au + Au collisions behave like a superposition of $p + p$ collisions with regard to high p_T π^0 production ($R_{AA} \approx 1$). In central collisions, the suppression is smallest at 2 GeV/c and increases to an approximately constant suppression factor of $1/R_{AA} \approx 4$–5 over the p_T range of 4–10 GeV/c, ~30% above the expectation from N_{part} scaling (dotted line in Fig. 2).

The magnitude and p_T dependence of R_{AA} (corresponding to parton fractional momenta $x \approx 2p_T/\sqrt{s} \sim 0.02$–$0.1$ at midrapidity) is inconsistent with the expectations of leading-twist "shadowing" effects on the nuclear parton distribution functions alone [25]. Different jet quenching calculations [4–7,10–12], based on medium-induced radiative energy loss, can reproduce the magnitude of the π^0 suppression assuming the formation of a hot and dense partonic system. The predicted p_T dependence of the quenching, however, varies in the different models. All models that include the Landau-Pomeranchuck-Migdal (LPM) interference effect [15,26] predict R_{AA} effectively $\propto \sqrt{p_T}$ [10]. Such a trend is not compatible with our data over the entire p_T range. Analyses which combine LPM jet quenching together with shadowing and initial-state p_T broadening generally reproduce the whole p_T dependence of the π^0 suppression [4], as do recent approaches that take into account detailed balance between parton emission and absorption [7]. However, based solely on the data presented here, we are not able to distinguish between partonic or hadronic [13] energy loss scenarios.

The centrality dependence of the high p_T π^0 suppression is shown in Fig. 3 as a function of $\langle N_{\mathrm{part}} \rangle$. The suppression is characterized as the ratio of Au + Au over $p + p$ yields integrated above 4 GeV/c and normalized using two different scalings. R_{AA} (circles) denotes the N_{coll} scaling as in Eq. (1), whereas R_{AA}^{part} (crosses) indicates N_{part} scaling expected in scenarios dominated either by gluon saturation [8] or by surface emission of the quenched jets [10]. Figure 3 indicates that the transition from the N_{coll} scaling behavior ($R_{AA} \sim 1$) apparent in the most peripheral region, to the strong suppression seen in central reactions ($R_{AA} \sim 0.25$) is smooth. In addition, although there is no exact participant scaling ($R_{AA}^{\mathrm{part}} > 1$ for all centralities), the π^0 production per participant pair above 4 GeV/c is approximately constant over a wide range of intermediate centralities, in qualitative agreement with a parton saturation model prediction [8].

In summary, transverse momentum spectra of neutral pions have been measured at midrapidity up to $p_T \approx 10$ GeV/c for nine centrality bins of Au + Au collisions at $\sqrt{s_{NN}} = 200$ GeV. The spectral shape and invariant yield for peripheral reactions are consistent with those of $p + p$ reactions scaled by the average number of inelastic NN collisions. Central yields, on the other hand, are significantly lower than peripheral Au + Au and $p + p$ scaled yields, as found at $\sqrt{s_{NN}} = 130$ GeV. The observed suppression increases slowly with p_T to as much as a factor of 4–5 in the 10% most central collisions,

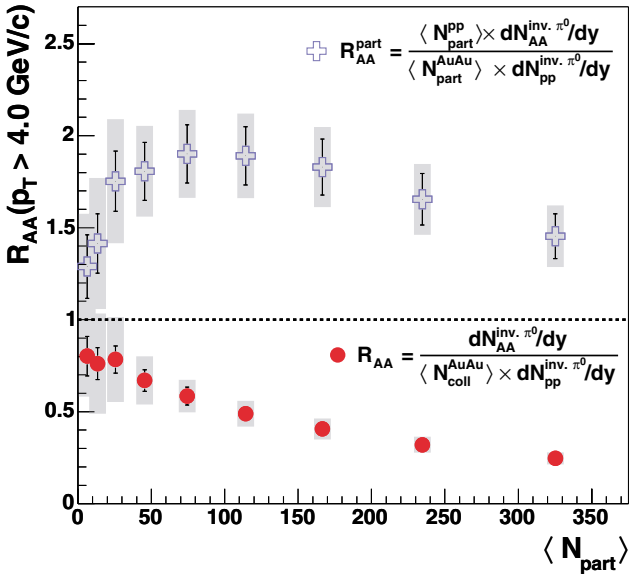

FIG. 3 (color online). Ratio of Au + Au over $p + p$ π^0 yields integrated above 4 GeV/c and normalized using $\langle N_{\mathrm{coll}} \rangle$ (circles) and $\langle N_{\mathrm{part}} \rangle$ (crosses), as a function of centrality given by $\langle N_{\mathrm{part}} \rangle$. The errors bands and bars are the same as for Fig. 2.

remaining constant within errors above ~ 4 GeV/c. The suppression is already apparent in semiperipheral reactions and increases smoothly with centrality. The magnitude of the deficit can be reproduced by parton energy loss calculations in an opaque medium, but its p_T and centrality dependence puts strong constraints on the details of energy loss and the properties of the medium. The role of initial-state effects, including shadowing, p_T broadening, and gluon saturation will be studied with data from the recent RHIC run using $d + \mathrm{Au}$, where final-state medium effects such as jet quenching are minimal.

We thank the staff of the Collider-Accelerator and Physics Departments at BNL for their vital contributions. We acknowledge support from the Department of Energy and NSF (U.S.A.), MEXT and JSPS (Japan), CNPq and FAPESP (Brazil), NSFC (China), CNRS-IN2P3 and CEA (France), BMBF, DAAD, and AvH (Germany), OTKA (Hungary), DAE and DST (India), ISF (Israel), KRF and CHEP (Korea), RMIST, RAS, and RMAE (Russia), VR and KAW (Sweden), U.S. CRDF for the FSU, U.S.-Hungarian NSF-OTKA-MTA, and U.S.-Israel BSF.

*Deceased.
†PHENIX Spokesperson.
Email address: zajc@nevis.columbia.edu

[1] See E. Laermann and O. Philipsen, hep-ph/0303042 [Annu. Rev. Nucl. Part. Sci. (to be published)], for a recent review.
[2] J. F. Owens *et al.*, Phys. Rev. D **18**, 1501 (1978).
[3] R. J. Glauber and G. Matthiae, Nucl. Phys. **B21**, 135 (1970).
[4] I. Vitev and M. Gyulassy, Phys. Rev. Lett. **89**, 252301 (2002).
[5] S. Jeon, J. Jalilian-Marian, and I. Sarcevic, Phys. Lett. B **562**, 45 (2003).
[6] G. G. Barnafoldi *et al.*, nucl-th/0212111.
[7] X. N. Wang, Nucl. Phys. **A715**, 775 (2003).
[8] D. Kharzeev, E. Levin, and L. McLerran, Phys. Lett. B **561**, 93 (2003).
[9] K. Adcox *et al.*, Phys. Rev. Lett. **88**, 022301 (2002).
[10] B. Müller, Phys. Rev. C **67**, 061901(R) (2003), and references therein.
[11] F. Arleo, J. High Energy Phys. 11 (2002) 044.
[12] C. A. Salgado and U. A. Wiedemann, Phys. Rev. D **68**, 014008 (2003).
[13] K. Gallmeister, C. Greiner, and Z. Xu, Phys. Rev. C **67**, 044905 (2003).
[14] M. Gyulassy and M. Plümer, Phys. Lett. B **243**, 432 (1990); X. N. Wang and M. Gyulassy, Phys. Rev. Lett. **68**, 1480 (1992).
[15] R. Baier, D. Schiff, and B. G. Zakharov, Annu. Rev. Nucl. Part. Sci. **50**, 37 (2000), and references therein.
[16] S. S. Adler *et al.*, hep-ex/0304038 (to be published).
[17] L. Aphecetche *et al.*, Nucl. Instrum. Methods Phys. Res., Sect. A **499**, 521 (2003).
[18] GEANT 3.21, CERN program library.
[19] X. N. Wang and M. Gyulassy, Phys. Rev. D **44**, 3501 (1991).
[20] K. Adcox *et al.*, Phys. Rev. Lett. **86**, 3500 (2001).
[21] The trigger is inefficient for very peripheral reactions and records $92.2^{+2.5}_{-3.0}\%$ of σ_{AuAu}.
[22] Woods-Saxon Au nuclear radius $R = 6.38 \pm 0.06$ fm, diffusivity $a = 0.535 \pm 0.027$ fm [B. Hahn, D. G. Ravenhall, and R. Hofstadter, Phys. Rev. **101**, 1131 (1956)], and nucleon-nucleon cross section $\sigma_{NN}^{\mathrm{inel}} = 42 \pm 3$ mb.
[23] M. M. Aggarwal *et al.*, Eur. Phys. J. C **23**, 225 (2002).
[24] D. Antreasyan *et al.*, Phys. Rev. D **19**, 764 (1979).
[25] K. J. Eskola, V. J. Kolhinen, and C. A. Salgado, Eur. Phys. J. C **9**, 61 (1999); S. R. Klein and R. Vogt, Phys. Rev. C **67**, 047901 (2003).
[26] M. Gyulassy, P. Levai, and I. Vitev, Phys. Rev. Lett. **85**, 5535 (2000); Nucl. Phys. **B594**, 371 (2001).